

## Finite element procedures for the numerical simulation of fatigue crack propagation under mixed mode loading

Abdulnaser M. Alshoaibi\*

*Department of Mechanical Engineering, Jazan University, Jazan, P.O. Box 706,  
Kingdom of Saudi Arabia*

*(Received October 20, 2009, Accepted January 22, 2010)*

**Abstract.** This paper addresses the numerical simulation of fatigue crack growth in arbitrary 2D geometries under constant amplitude loading by the using a new finite element software. The purpose of this software is on the determination of 2D crack paths and surfaces as well as on the evaluation of components Lifetimes as a part of the damage tolerant assessment. Throughout the simulation of fatigue crack propagation an automatic adaptive mesh is carried out in the vicinity of the crack front nodes and in the elements which represent the higher stresses distribution. The fatigue crack direction and the corresponding stress-intensity factors are estimated at each small crack increment by employing the displacement extrapolation technique under facilitation of singular crack tip elements. The propagation is modeled by successive linear extensions, which are determined by the stress intensity factors under linear elastic fracture mechanics (LEFM) assumption. The stress intensity factors range history must be recorded along the small crack increments. Upon completion of the stress intensity factors range history recording, fatigue crack propagation life of the examined specimen is predicted. A consistent transfer algorithm and a crack relaxation method are proposed and implemented for this purpose. Verification of the predicted fatigue life is validated with relevant experimental data and numerical results obtained by other researchers. The comparisons show that the program is capable of demonstrating the fatigue life prediction results as well as the fatigue crack path satisfactorily.

**Keywords:** finite element simulation; stress intensity factors; mixed mode fracture; adaptive mesh; fatigue life prediction.

---

### 1. Introduction

Fatigue damage accumulation can be explained in terms of the initiation and growth of small cracks in the metal. The crack propagation progressively reduces the capability of the components to withstand the applied external load and finally break the components. The analysis of fatigue crack growth is essential to ensure the reliability of structures under cyclic loading conditions. Cracks, as a result of manufacturing defects or localized damage, may extend until brittle fracture occurs. In linear elastic fracture mechanics, cracks initiation is not considered. The major source of failure of structural components is fatigue crack growth. In the past, the S-N curves were the only engineering tools, and crack propagation was not considered to predict lifetime. Nevertheless, at

---

\*Ph.D., E-mail: [alshoaibi@gmail.com](mailto:alshoaibi@gmail.com)

present, studying crack growth behaviour has been made possible by the LEFM and the prediction of remaining lifetime of components is accessible. This is of great practical importance in order to know if a part can be still used or must be replaced.

A predictive method consists of computing the crack driving force and integrating the crack growth law. Two kinds of data are required: first, the experimental Paris crack growth law of the considered material and second, the stress intensity factors (SIFs) distribution along the crack front. The Paris relation is quite easy to obtain on the contrary to SIFs (Courtin *et al.* 2005).

A number of equations have been developed to describe the sigmoidal  $da/dN-\Delta K$  relationship. Paris and Erdogan (1960) were apparently the first to discover the power law relationship to describe the stable crack growth. Many variations based on the Paris law have been developed to consider the  $R$ -ratio effect, the threshold value of the stress intensity factor range ( $\Delta K_{th}$ ), and the fracture toughness of the material ( $K_c$ ) (Fpreman *et al.* 1967, Weertman 1966, Klesnil and Lukas 1972, McEvily 1988).

Since the fatigue crack growth rate is mainly controlled by the stress intensity factor range,  $\Delta K$ , and the maximum stress intensity factor,  $K_{max}$  (Zhao *et al.* 2008).

Various attempts have been made to develop efficient models to estimate fatigue crack growth and life time. The analytical approach, such as that contained in NASCRAC and NASA/FLAGRO for fatigue crack growth, employs known solutions for  $K_I$  as a function of crack length to generate crack growth predictions. Such predictions are therefore limited to self-similar crack growth. Further, the analytical solutions are available for only a limited set of combinations of geometries and boundary conditions.

However, several simulation codes have already been developed for the evaluation of cracks within 2D components, e.g., FRAN2D, FASTRAN (Newman 1981, 1992), AFGROW and NASGRO. In addition, there are many recent development performed by many researchers to find an efficient method to predict the fatigue crack growth under mixed mode loading in 2D linear elastic structures e.g., (Lebaillif and Recho 2007, Yan 2007, DufLOT and Dang 2004).

The present software code has been developed to enable the user to determine 2D-cracks under mixed mode loading and, with the aid of automatic adaptive mesh finite element, to analyst fatigue crack path lifetimes. This program is written in FORTRAN language. The finite element calculations provided by this software produce results comparable to the current available commercial software. Use of commercial code for research applications is difficult for two reasons first, the fundamental algorithm that lies behind it is not fully comprehended and secondly the state of art in the programming skill is absolutely in apprehended.

## 2. The simulation model

The finite element procedure usually consists of three main parts namely pre-processing, processing and post-processing. The finite element processing is often considered as the most time consuming part in the computation. This part contains the evaluation and assembly routine for the equation stiffness matrices and the system solver. The developed code is simulation software for the evaluation of 2D crack growth processes under general mixed-mode loading conditions. Based on the finite element (FE) method and under consideration of fracture mechanical boundary conditions this software predicts quasi-static fatigue crack growth in 2D components.

Throughout the simulation of crack propagation an automatic adaptive mesh is carried out in the

vicinity of the crack front nodes and in the elements which represent the higher stresses distribution. The finite element mesh is generated using the advancing front method. In order to suit the requirements of the fracture analysis, the generation of the background mesh and the construction of singular elements have been added to the developed program.

The adaptive remeshing process carried out based on the posteriori stress error norm scheme to obtain an optimal mesh adopted from Alshoaibi *et al.* (2007). The program adopted a frontal solver which is an efficient direct solver used to solve the system of linear equations.

### 3. Stress intensity factor and fatigue crack growth analysis

In this paper, the displacement extrapolation technique (Phongthanapanich and Dechaumphai 2004) is used to calculate the stress intensity factors as follows

$$K_I = \frac{E}{3(1 + \nu)(1 + \kappa)\sqrt{L}} \left[ 4(v'_b - v'_d) - \frac{(v'_c - v'_e)}{2} \right] \tag{1}$$

$$K_{II} = \frac{E}{3(1 + \nu)(1 + \kappa)\sqrt{L}} \left[ 4(u'_b - u'_d) - \frac{(u'_c - u'_e)}{2} \right] \tag{2}$$

where  $E$  is the modulus of elasticity,  $\nu$  the Poisson’s ratio,  $\kappa$  an elastic parameter equal to  $3 - 4\nu$  for plane strain and  $(3 - \nu)/(1 + \nu)$  for plane stress and  $L$  is the length of the element side connected to the crack tip. The near tip nodal displacements at nodes  $b, c, d$  and  $e$  shown in Fig. 1 are of interest. The displacement tangential and normal to crack plane is denoted as  $u'$  and  $v'$  respectively.

In order to simulate fatigue crack propagation under LEFM condition, the crack path direction must be predicted. There are several methods used to predict the direction of the crack trajectory such as maximum circumferential stress theory, maximum energy release rate theory and minimum strain energy density theory. Here the maximum circumferential stress criterion is chosen due to its simplicity. This theory asserts that, for isotropic materials under mixed-mode loading, the crack will

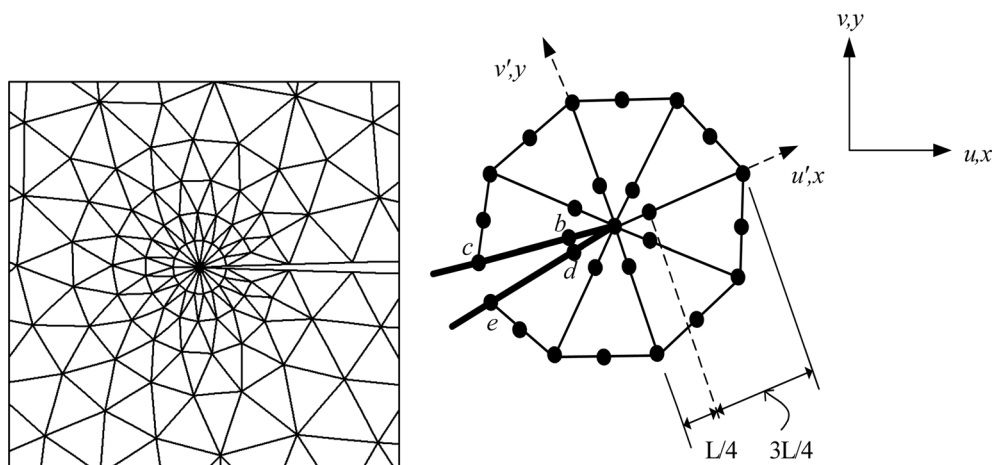


Fig. 1 Quarter-point singular elements around the crack tip

propagate in a direction normal to maximum tangential tensile stress. In polar coordinates, the stresses at the crack tip for mode I and II are given by

$$\begin{aligned}\sigma_r &= \frac{1}{\sqrt{2\pi r}} \cos(\theta/2) \left( K_I [1 + \sin^2(\theta/2)] + \frac{3}{2} K_{II} \sin \theta - 2K_{II} \tan(\theta/2) \right) \\ \sigma_\theta &= \frac{1}{\sqrt{2\pi r}} \cos(\theta/2) \left[ K_I \cos^2(\theta/2) - \frac{3}{2} K_{II} \sin \theta \right] \\ \tau_{r\theta} &= \frac{1}{\sqrt{2\pi r}} \frac{\cos(\theta/2)}{2} [K_I \sin \theta + K_{II} (3 \cos \theta - 1)]\end{aligned}\quad (3)$$

where  $\sigma_r$  is the normal stress component in the radial direction,  $\sigma_\theta$  is the normal stress component in the tangential direction and  $\tau_{r\theta}$  is the shear stress component. The direction normal to the maximum tangential stress can be obtained by solving  $d\sigma_\theta/d\theta = 0$  for  $\theta$ . The nontrivial solution is given by

$$K_I \sin \theta + K_{II} (3 \cos \theta - 1) = 0 \quad (4)$$

which can be solved as

$$\theta = 2 \arctan \left( \frac{1}{4} \frac{K_I}{K_{II}} \pm \frac{1}{4} \sqrt{\left( \frac{K_I}{K_{II}} \right)^2 + 8} \right) \quad (5)$$

In order to ensure that the opening stress associated with the crack direction of the crack extension is maximum, the sign of  $\theta$  should be opposite to the sign of  $K_{II}$  (Andersen 1998). The two possibilities are illustrated in Fig. 2.

Since fatigue is a cyclic dissipation of energy in the form of hysteretic loops, it is a cumulative damage process. The elapsed time for damage is expressed in term of the number of fatigue cycles ( $N$ ). This process is defined by crack growth per cycle;  $da/dN$ . The rate  $da/dN$  depends on the applied stress intensity factor range. Basically, for fatigue crack to grow, the resulted stress intensity range at each crack tip must exceed the stress intensity threshold defined as

$$\Delta K_{th} = f \Delta \sigma_{th} \sqrt{\pi a} \quad (6)$$

where  $f$  is a function of geometry and loading and  $\Delta \sigma_{th}$  is the stress range limit. Eq. (6) set a criterion whereby fatigue crack does not propagate if  $\Delta \sigma < \Delta \sigma_{th}$ . However, practically a parameter

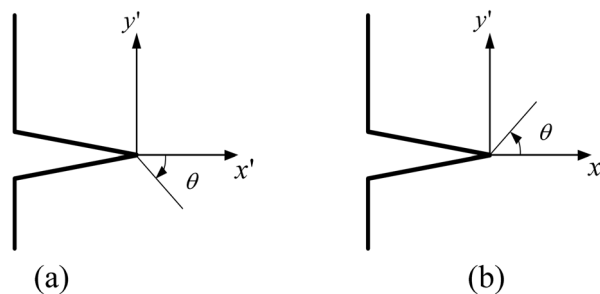


Fig. 2 Sign of the propagation angle (a)  $K_{II}$  positive and (b)  $K_{II}$  negative

known as equivalent stress intensity factor range,  $\Delta K_{Ieq}$ , is used as indicator for fatigue crack propagation. In such  $\Delta K_{Ieq} > \Delta K_{Ith}$  indicates that fatigue crack growth will happen otherwise there is no fatigue crack propagation. An equivalent stress intensity factor  $K_{Ieq}$  is given by the maximum hoop stress criterion (see, e.g., Broek 1982)

$$\Delta K_{Ieq} = \Delta K_I \cos^3(\theta/2) - 3\Delta K_{II} \cos^2(\theta/2) \sin(\theta/2) \tag{7}$$

Thus it is easy to model the stable crack propagation using the generalized Paris' equation as

$$\frac{da}{dN} = C(\Delta K_{Ieq})^m \tag{8}$$

where  $C$  and  $m$  are the material properties.

Eq. (8) was developed on the assumption that a) the plastic deformation due to cyclic tension and transfer shear are not interactive, and b) the resulting displacement field is the sum of the displacements from the two modes.

Tanaka (1974) carried out experiments on cyclical loaded ( $R = 0.65$ ) sheets of pure aluminum with initial cracks inclined to the tensile axis. The general purpose of the study was to establish threshold bounds for cyclic mixed mode fatigue crack growth. He proposed the following formula for the equivalent stress intensity factor

$$\Delta K_{Ieq} = [\Delta K_I^4 + 8\Delta K_{II}^4]^{0.25} \tag{9}$$

This formula is equivalent to that obtained in Eq. (7). The number of cycles  $N_{if}$  can be predicted for the crack propagation by integrating from the initial length  $a_i$  to the final crack length  $a_f$  as

$$N_{if} = \int_{a_i}^{a_f} \frac{1}{C(\Delta K_{Ieq})^m} da \tag{10}$$

For a single-cracked body case,  $\Delta a$ , can be substituted directly into the piece wise numerical integration. For fatigue crack propagation analysis, the master structure of the program has to be outlined to have a clear picture on how such every stage of the programming should be organized. The computational scheme which is used to simulate fatigue crack propagation is illustrated in Fig. 3. The main stages of this scheme are illustrated as follows:

1. The input files of the program must contains the 2D geometry domain of the problem, constraint and loading, material properties and pre-crack nodes, which were defined by the user. Using the information from pre-crack nodes list, the rosette templates can be cut out and subsequently the background mesh is generated. The strategy taken to generate the background mesh is to utilize all the initial boundary nodes or only the external boundary nodes of geometry and construct the boundary triangles as the background mesh by the dichotomy technique (Alshoaibi *et al.* 2007). This background mesh, serves to control the distribution of the mesh parameters during the actual mesh generation by the advancing front method (Zienkiewicz *et al.* 2005). Subsequently, the 3 nodes triangle mesh is generated over the whole domain but of course excluding the rosette template. Consequently the mesh smoothing procedure as prescribed by Zienkiewicz *et al.* (2005) is employed to enhance the mesh quality.
2. Subsequently the triangles for the rosette elements are generated. In order to have six nodes triangles, a mid side node is added to each triangle edge, but for the rosette elements, the mid side nodes for the triangle edges that connected to the crack tip are shifted to the quarter length of the edges nearer to the crack tip.

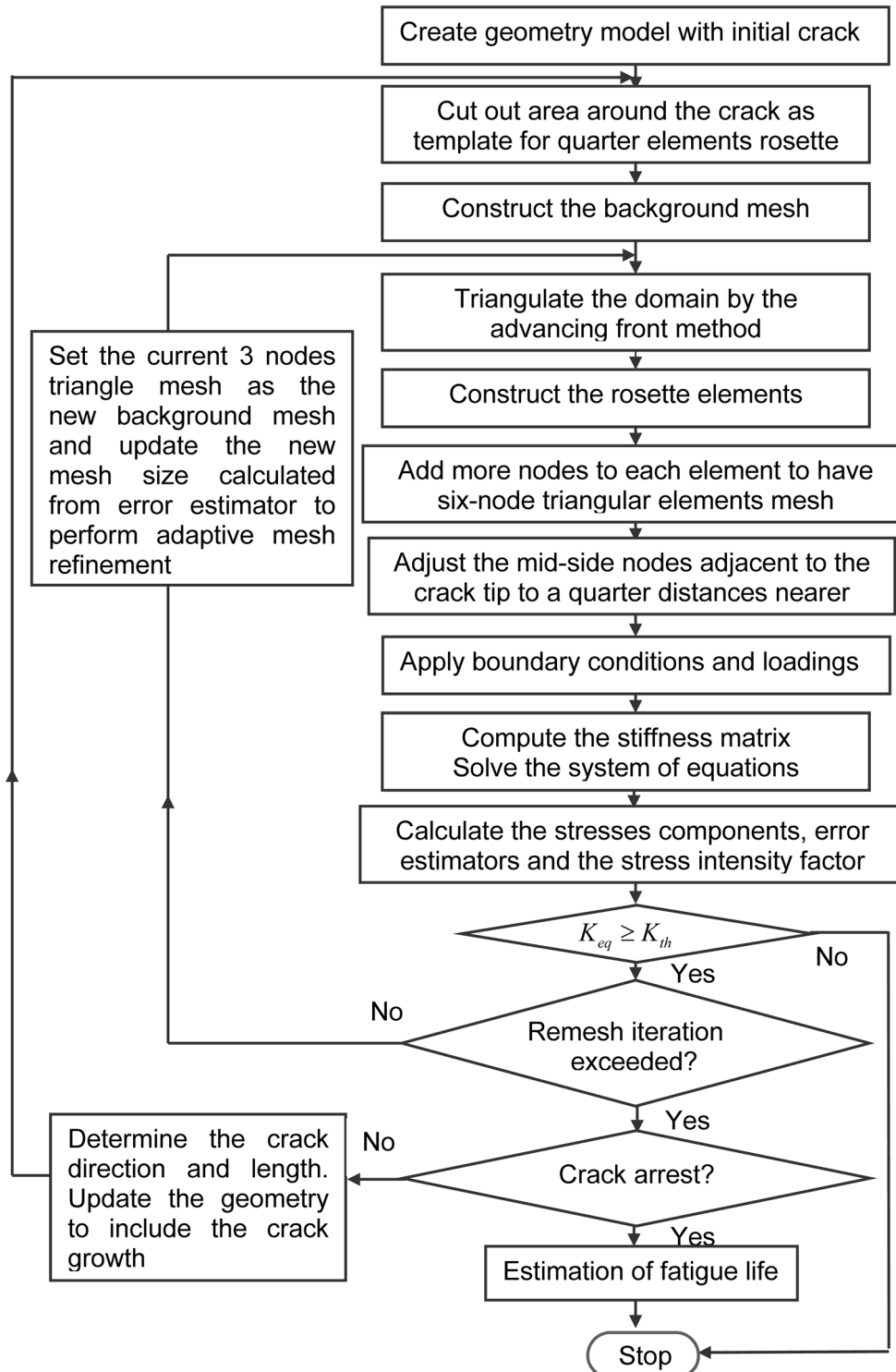


Fig. 3 Computational scheme of the fatigue crack propagation program

In the implementation, the nodes numbering are also optimized in such, nodes which are nearer to each other have a closer numbering sequence. This special quarter point elements are used to capture the stress-strain singularity at the crack tip.

3. The user input file containing the constraints and loadings data is read. The prescriptions initially based on the original boundary segments and nodes. Since during the meshing procedure more boundary nodes has been added and including also the mid side nodes of the triangles which may lay on the boundary segments and furthermore the new numbering sequence adopted, mapping from old numbering boundary nodes to the new one with respect to the constraints and loadings has to be conveyed.
4. The stiffness matrix is then evaluated and store in file storage, element by element. At this stage we have the system of equations consist of the stiffness matrix of each element at the left hand side and the nodal representation of forces at the right hand side waiting to be assembled and solved. Use of the frontal solver has the advantage that it does not require complete assembly of the global stiffness matrix.
5. From the frontal solver solutions, displacements, strains and stresses can be determined for each node.
6. The adaptive mesh refinement is employed as the optimization scheme. This scheme is based on a posteriori error estimator which is obtained from the solution of the previous mesh. The error estimator based on the norm stress error must be evaluated in order to adaptively refine the mesh by determining the optimize element size for the next new mesh as explained in details by Foreman *et al.* (1967). In the mean while the stress intensity factors can be calculated as well. The iteration for refinement process can be either controlled by the convergence of stress intensity factor (Phongthanapanich and Dechaumphai 2004) or just by considerably setting number of iteration needed.
7. After that, the equivalent SIF ( $\Delta K_{eq}$ ) at the last refinement iteration is compared to the threshold stress intensity factor  $\Delta K_{th}$ . If  $\Delta K_{eq} \geq \Delta K_{th}$  then the crack will propagate from the respective crack tip to a certain direction with a certain length as explained in the previous section.
8. The next step is to determine whether the crack is likely to propagate, and if so, in which direction. The maximum circumferential stress criterion is used to predict the crack propagation direction, as explained previously. The next step is to locate the position of the new crack tip using nodal splitting and relaxation as will clarify in section 4. Based on the stress criterion of the crack opening, the crack can grow only when the compressive stresses at the crack tip are released (Lebaillif and Recho 2007).
9. If at least one of the pre cracks grows then the geometry, constraints and loading of the structure need to be updated before the process is repeated.
10. The developed program has safety features to automatically stop the calculation if, during any loading event, it detects that: (i)  $K_{Ieq,max} = K_{Ic}$ ; (ii) the crack has reached its maximum specified size; (iii) one of the borders of the piece is reached by the crack front; (iv)  $(da/dN)$  reaches 0.1 mm/cycle (for most engineering alloys, above this rate the problem is fracturing, not fatigue cracking (Miranda *et al.* 2003). These conditions are checked in the computational scheme chart under the crack arrest condition block.
11. The program will directly predict the fatigue life cycles after the stress intensity factors and crack propagation length histories are completely recorded. The integration in Eq. (10) is carried out numerically by employing piecewise trapezoidal algorithm.

#### 4. Node splitting and relaxation

The opening of the new crack segment, which up to this point was closed, is done by splitting and releasing the nodes along its faces. At this stage the unbalance is only due to the nonzero nodal forces acting on both sides of the new crack segment. These nodal forces were self-equilibrating as long as the crack segment was closed, but become external forces upon nodal splitting and are no longer in equilibrium with the new boundary conditions. When the condition of crack growth is satisfied at the particular crack tip then the node at the crack tip has to be split into two nodes to simulate the crack opening. Before that the displacement must be updated to the boundary node coordinates if need to show the deformation. The length of the splitting is set by the user but must be very small value. The direction of the splitting is taken upwards and downwards at the half of the angle between the segment that firstly contains the current crack tip and the segment that connecting the current crack tip to the approximated next crack tip. This direction is taken in order to avoid interception between the new boundary lines and the updated existence boundary lines.

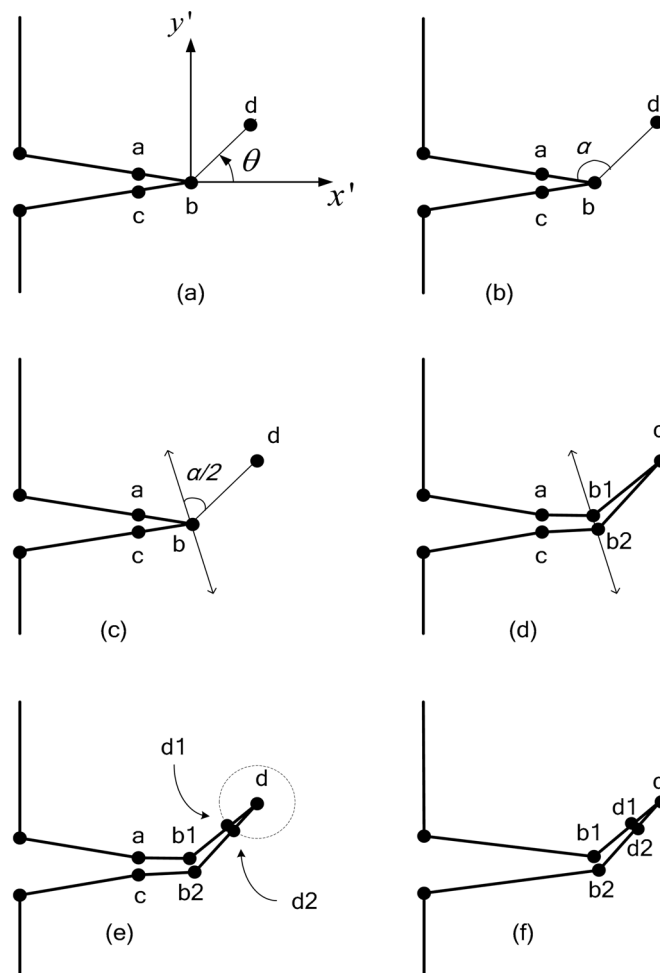


Fig. 4 Splitting of crack node and boundary nodes updating procedure

Fig. 4 illustrates the procedure of the splitting crack tip node. Let say  $a$  and  $c$  are the first nodes before and after the crack tip  $b$  respectively while  $d$  is the approximated next crack tip with the incremental crack length  $|bd|$  and the direction  $\theta$  as shown in Fig. 4(a).

The length of crack-extension increments was found not to influence results of stress intensity factors for increments below 5% of the initial crack length (Tilbrook *et al.* 2005). The angle  $\alpha$  between segment  $ab$  and  $bd$  is being considered as in Fig. 4(b). The direction of splitting is then taken at  $\alpha/2$ , where both upwards and downwards direction are involved as shown in Fig. 4(c). In this case if  $\Delta s$  is set as the length of the splitting then the length of each split nodes  $b_1$  and  $b_2$  from the initial crack tip will be  $\Delta s/2$ . The final splitting process is shown in Fig. 4(d).

Notice that in this work, there is no precise information on how to ‘naturally’ determine the length and direction of the splitting. The technique used here is based from two naive assumptions which are first, the length of the splitting should be not larger than the distance of the first two neighboring boundary nodes (for instance  $|ac|$  in Fig. 4(a)) and second, the direction should avoid intersection of the straight segments from occurring which can be seen as merely a geometrical factor. These assumptions are matched with other assumptions proposed by other researchers (e.g., Mediavilla *et al.* 2006, Paluszny *et al.* 2009).

The relaxation of the split nodes means the nodes are released according to the mechanical properties. As being mentioned in the previous paragraph, this is momentarily being ignored until it comes to next computational process where the displacement of the points (for example, the current  $b_1$  and  $b_2$  in Fig. 4) allocates them following the constitutive law of the system. If the new segments connecting the new crack tip to the split nodes do not have the same length then it will be impossible to create the uniform rosette template later. For example in Fig. 4(d) if the length of segment  $b_1d$  is taken as the radius for the rosette template then one more boundary point has to be added on segment  $b_2d$  in order to have the circular template as shown in Fig. 1. In this case the new radius for template which is also the next length for the singular element is defined as  $L = \Delta a/10$ . Therefore two more boundary nodes are going to be added as shown in Fig. 4(e). However in our implementation there are also two boundary nodes were deleted i.e., the first nodes before and after the previous crack tip in the list which are actually added to serve as indicators for setting up the rosette circle. Furthermore, those two nodes, are set very near to the crack tip therefore it is assumed that removing points  $a$  and  $c$  does not significantly affect the shape of the geometry and hence the accuracy of the calculation.

Finally only total of three nodes added in each crack propagation step instead of five as depicted in Fig. 4(f) and the geometry now can be updated. One can see that in the next propagation step nodes  $b_1$  and  $b_2$  in Fig. 4(f) will also be removed. It should be reminded that the quarter point nodes as well as the mid side nodes of the elements at this moment are not included as the boundary nodes even though they may lay on the boundaries. The constraint, loading and crack tip listing also need to be updated accordingly concerning the addition of new boundary segments in order to repeat the process from the beginning.

## 5. Numerical results and validation

### 5.1 Modified four point bending SEN specimen

The crack pattern for mixed mode fracture is usually a curve. It is of interest to investigate fatigue

crack growth behavior for such case. For this purpose, a modified four point bending is tested under constant amplitude fatigue loading with load ratio,  $R = \sigma_{\min}/\sigma_{\max} = 0.1$  with a maximum value of 250 KN.

Fig. 5 shows the dimensions of the modified four-point bending SEN and the final adaptive mesh for the first step. The material for this specimen is steel with the following properties:  $E = 205$  GPa,  $\nu = 0.333$ ,  $\sigma_y = 285$  MPa,  $\Delta K_{th} = 11.6$  MPa $\sqrt{m}$ ,  $C = 4.5 \times 10^{-10}$  and  $m = 2.1$ .

Fig. 6 shows four different steps of fatigue crack propagation of this specimen.

The experimental and numerical results obtained by Miranda *et al.*, Fig. 7, are used for comparison in the current work (Miranda *et al.* 2003).

One can obviously observe the similarity of crack path pattern predicted in the present study and those obtained in Fig. 6.

For more clarify of the accuracy of the crack path prediction, Fig. 8(a) shows the crack path with the maximum principal stress distribution and also the enlargement of the contour area around the crack tip. As shown in Fig. 8(b) the higher stress is concentrated at the crack tip and the crack path is almost similar to the experimental path obtained by Miranda *et al.* (2003).

Fig. 9 shows comparison of the stress intensity factor,  $K_I$ , which has been normalized to a geometry function,  $f(a/W)$  for this specimen, between the result of present study and the numerical result using Quebra2D obtained by Miranda *et al.* 2003. The geometry function for a standard SEN specimen in a close form solution can be obtained from Broek (1988) which also included in Fig. 9. It can be observed that the hole has a significant influence in the  $f(a/W)$  value, as well as the stress intensity factor. It is a satisfaction agreement between the present results and numerical results using

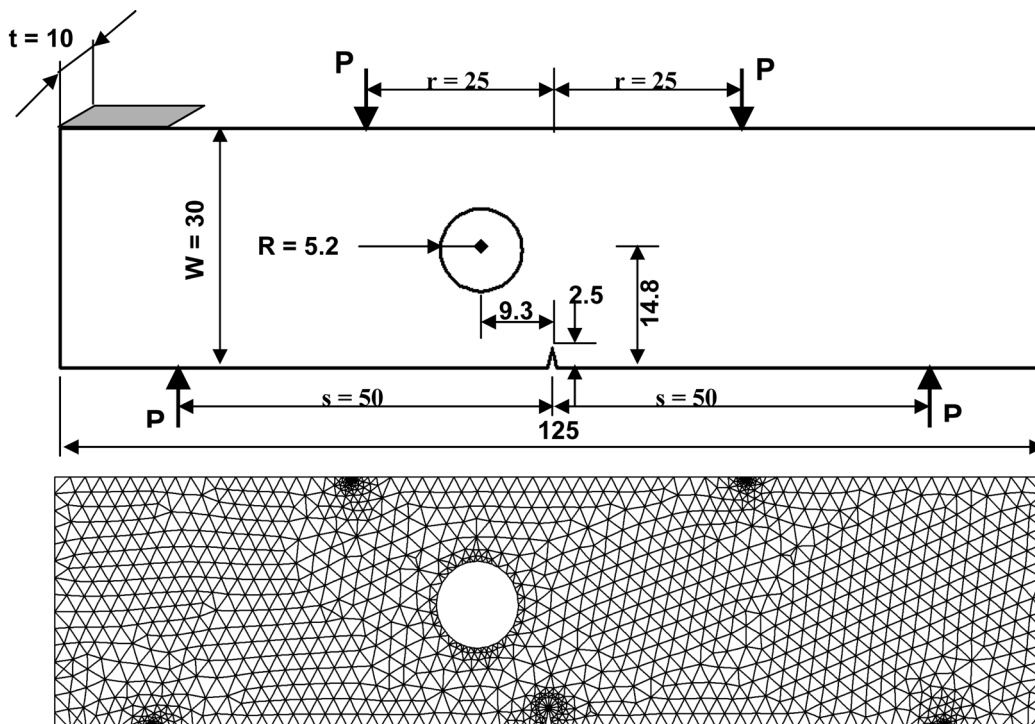


Fig. 5 Geometry of the modified SEN specimen (dimensions in mm) and final adaptive mesh

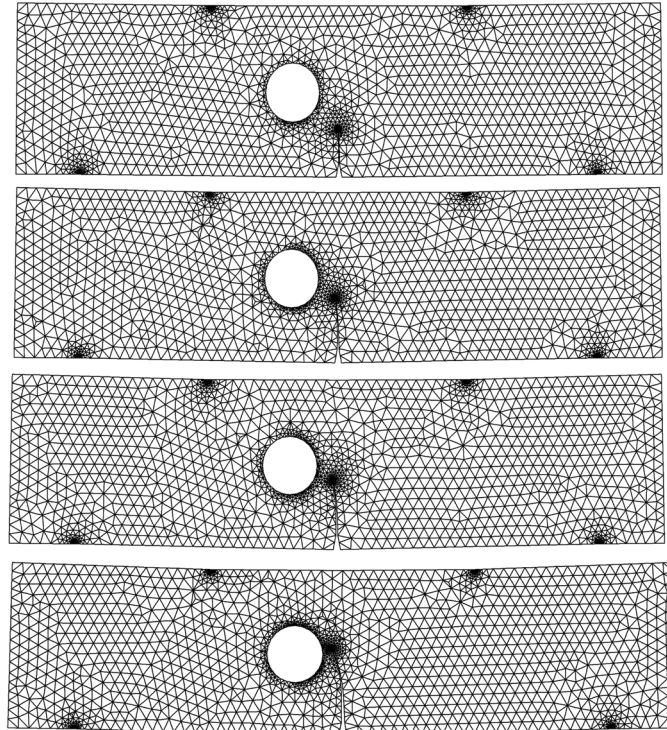


Fig. 6 Four steps of fatigue crack propagation of modified four-point bending SEN specimen

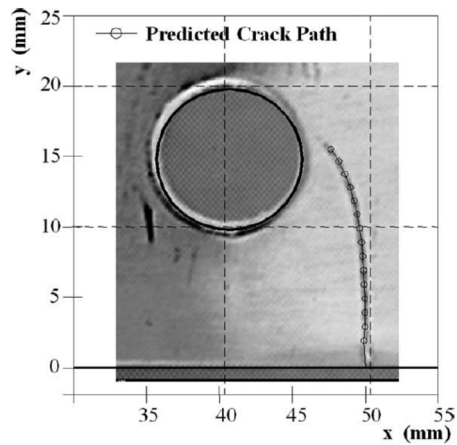


Fig. 7 Predicted and experimental crack path for the modified four-point bending SEN specimen by Miranda *et al.* (2003)

Quebra2D. The fatigue life diagram of this specimen is presented in Fig. 10. The life of the structure is evaluated as 653604 cycles, which is in agreement with experimental and numerical results using ViDa software obtained by Miranda *et al.* (2003).

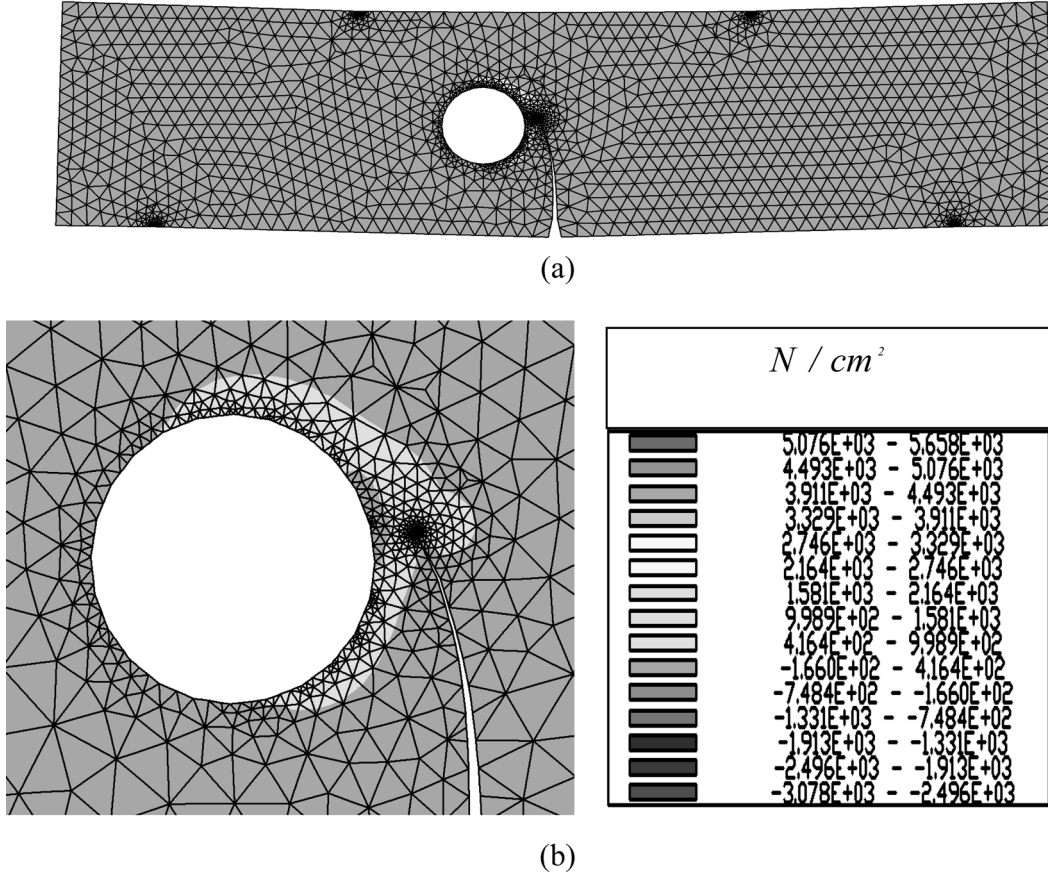


Fig. 8 (a) Crack trajectory and maximum principal stress distribution for the modified four-point bending SEN specimen (b) enlargement of the contour around crack tip

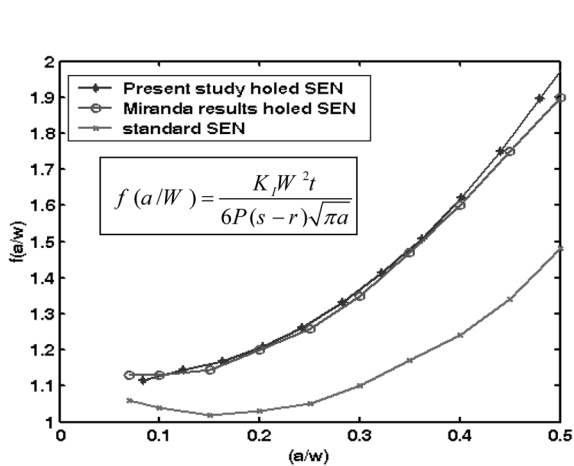


Fig. 9 Comparisons of the calculated  $f(a/w)$  expressions for the standard and modified four-point bending SEN specimen

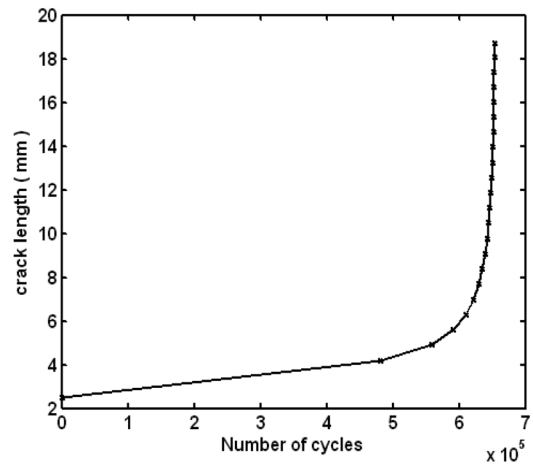


Fig. 10 Fatigue life diagram of the modified four point bending SEN specimen

5.2 Modified compact tension specimens

The modified CT specimens of two different geometries have been tested; each one has a 7 mm diameter hole positioned at a slightly different horizontal distance  $A$  and vertical distance  $B$  from the notch root, as shown in Fig. 11. This odd configuration was chosen because two non-trivial and unexpected crack growth behaviors had been observed depending on the location of the hole.

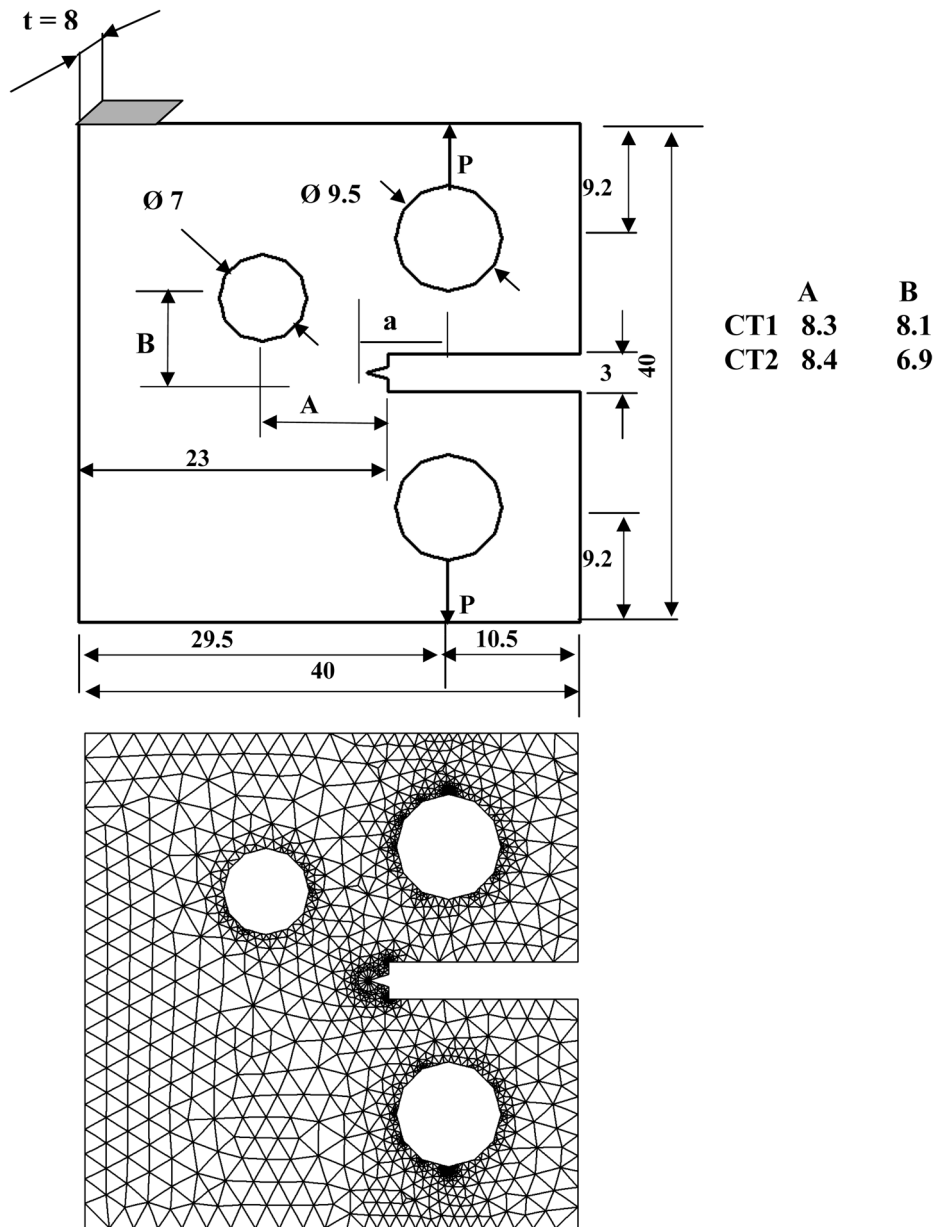


Fig. 11 Geometry of the modified CT specimens (dimensions in mm) and the final adaptive mesh

The material type of this specimen is taken as steel (same properties with the modified four point bending SEN specimen) and the applied load ratio  $R = 0.1$  with a maximum value of 250 KN. The computed  $K_I$  that has been normalized to  $f(a/w)$ , values are presented and compared to the standard CTS values and to numerical results obtained by Miranda *et al.* (2003) using Quebra2D software as

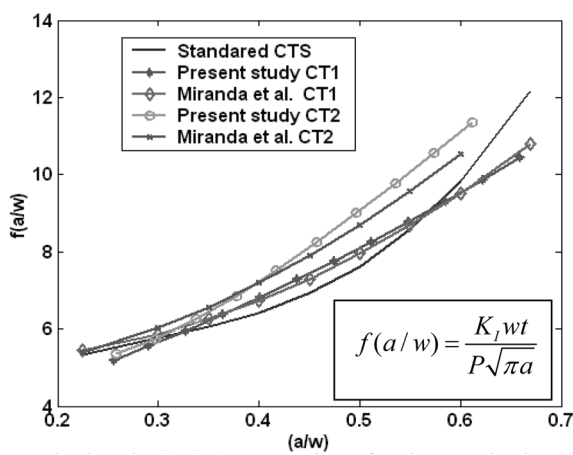


Fig. 12 Calculated  $f(a/w)$  expressions for the standard and for modified CT Specimens

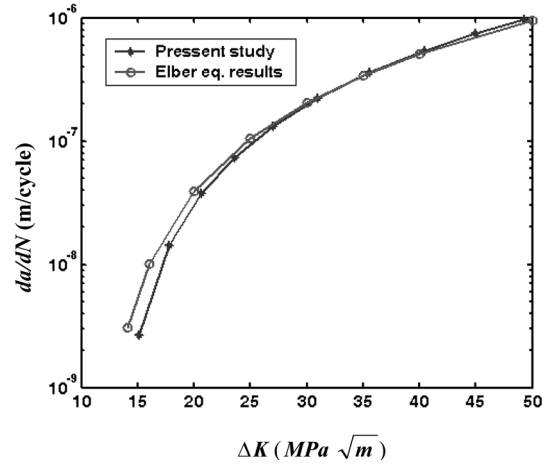


Fig. 13 Comparison for  $da/dN$  vs.  $\Delta K$  for CT2 specimen

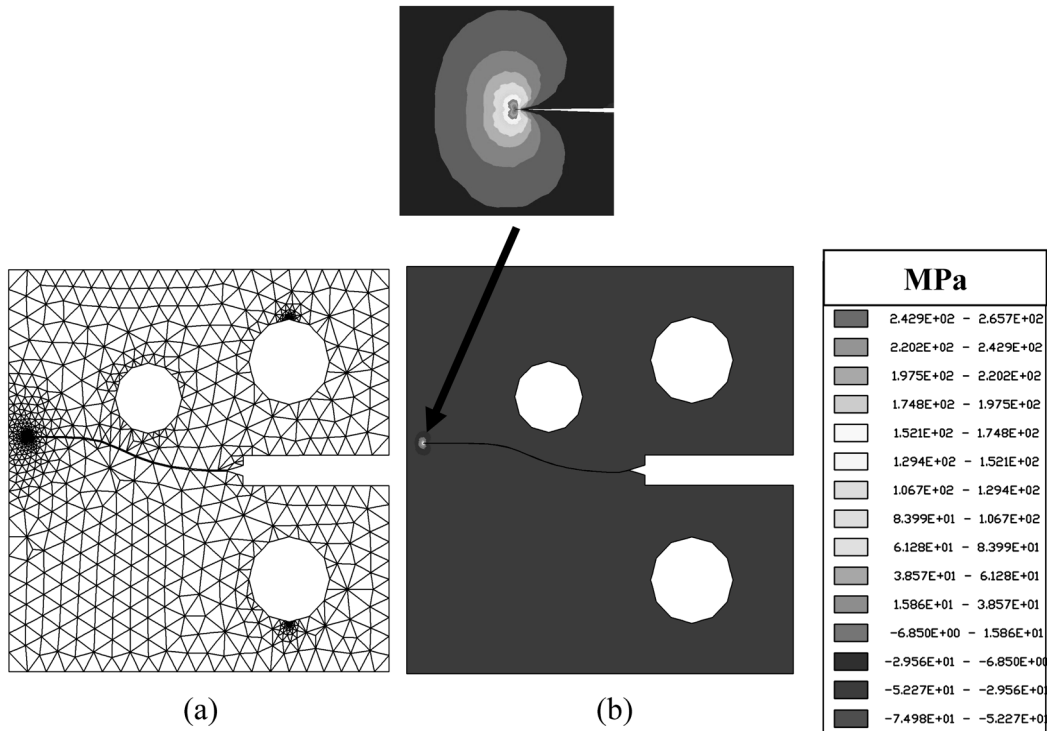


Fig. 14 (a) Final adaptive mesh of CT1 and (b) maximum principal stress

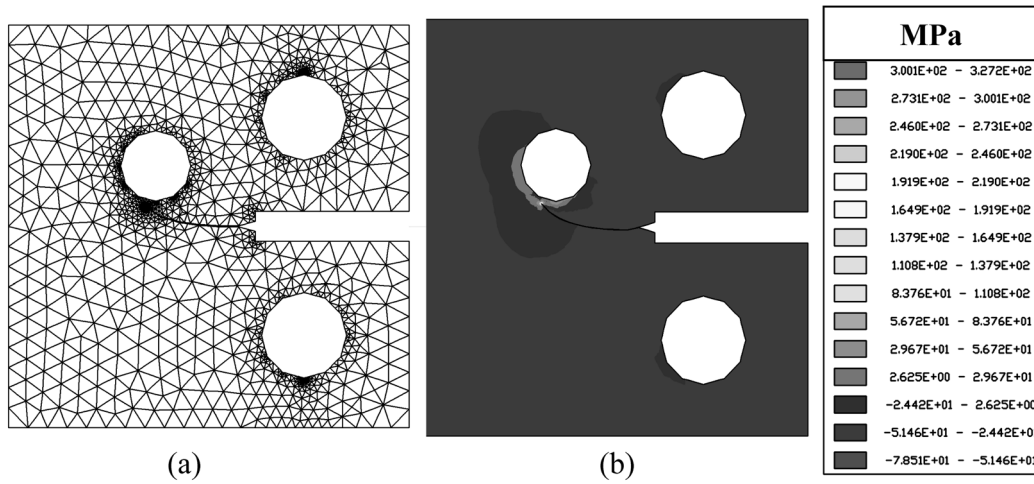


Fig. 15 (a) Final adaptive mesh of CT2 and (b) maximum principal stress

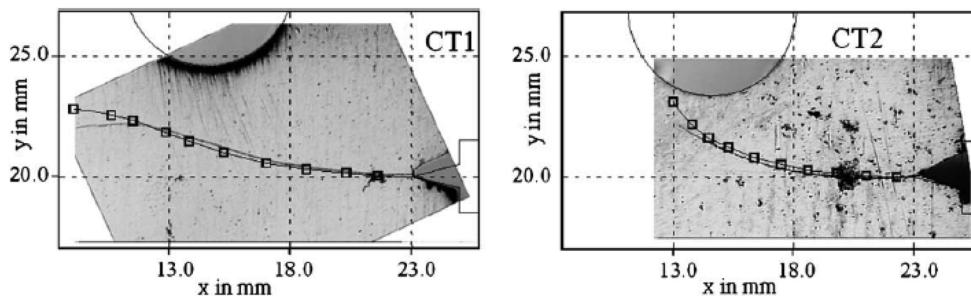


Fig. 16 Predicted and experimental crack path for the modified CT specimen obtained by Miranda *et al.* (2003)

shown in Fig. 12. As shown in this figure the agreements are obviously good.

Miranda *et al.* (2003) fitted their experimental data for fatigue life cycles of CT2 by Elber equation ( $da/dN = 4.5 \times 10^{-10} (\Delta K - \Delta K_{th})^{2.1}$ ). Comparison of the present result with the fitted equation for the fatigue life ( $da/dN$ ) versus  $\Delta K$  is shown in Fig. 13 with a good agreement.

The predicted crack path behaviors by the present developed program are shown in Figs. 14(a) and 15(a) for CT1 and CT2 respectively. Figs. 14(b) and 15(b) are representing the maximum principal stress distribution for CT1 and CT2 respectively. The predicted crack path behaviors are compared with those predicted experimentally and numerically using Quebra2D software by Miranda *et al.* (2003), as shown in Fig. 16. The crack paths predicted in the present study for both cases are very similar to those represented in Fig. 16.

The predictions indicate that the fatigue crack was always attracted by the hole, but it could either curve its path and grows toward the hole (“sink in the hole” behaviour) or just be deflected by the hole and continue to propagate after missing it (“miss the hole” behaviour).

## 6. Conclusions

The presented developed software is a powerful tool for the simulation of 2D crack propagation processes. The methodology developed for simulating automatic fatigue crack propagation in 2D structural components has been proven very practical and robust. The developed code is assessed with several test specimens and the outcomes are compared to the similar works either by numerically or experimentally; some of which were found in literatures and recent publications. Moreover, the developed software demonstrated that effective and economical prediction of crack propagation paths and fatigue lives can be obtained for arbitrary 2D structural components under constant amplitude loading.

## References

- Alshoaibi, M. Abdulnaser, M.S.A. Hadi and Ariffin, A.K. (2007), "Two-dimensional numerical estimation of stress intensity factors and crack propagation in linear elastic analysis", *J. Struct. Durability and Health Monitoring (SDHM)*, **3**(1), 15-27.
- Andersen, M.R. (1998), *Fatigue Crack Initiation and Growth in Ship Structures*, Ph.D Dissertation, Technical University of Denmark.
- Broek, D. (1988), *The Practical Use of Fracture Mechanics*, Kluwer Academic Publishers, Dordrecht.
- Broek, D. (1986), *Elementary Engineering Fracture Mechanics*, 4th Edition, Martinus Nijhoff Publishers, Dordrecht.
- Courtin, S., Gardin, C., Bezine, G. and Hamouda, H.B.H. (2005), "Advantages of the J-integral approach for calculating stress intensity factors when using the commercial finite element software ABAQUS", *Eng. Fract. Mech.*, **72**, 2174-2185.
- Duflot, M. and Dang, H.N. (2004), "Fatigue crack growth analysis by an enriched meshless method", *J. Comput. Appl. Math.*, **168**, 155-164.
- Foreman, R.G., Keary, V.E. and Engle, R.M. (1967), "Numerical analysis of crack propagation in cyclic-loaded structures", *J. Basic Eng.*, **89**, 459-464.
- Klesnil, M. and Lukas, P. (1972), "Influence of strength and stress history on growth and stabilization of fatigue cracks", *Eng. Fract. Mech.*, **4**, 77-92.
- Lebaillif, D. and Recho, N. (2007), "Brittle and ductile crack propagation using automatic finite element crack box technique", *Eng. Fract. Mech.*, **74**, 1810-1824.
- McEvily, A.J. (1988), *On Closure in Fatigue Crack Growth*, ASTM STP 982, American Society for Testing and Materials, Philadelphia.
- Mediavilla, J., Peerlings, R.H.J. and Geers, M.G.D. (2006), "A robust and consistent remeshing-transfer operator for ductile fracture simulations", *Comput. Struct.*, **84**, 604-623.
- Miranda, A.C.O., Meggiolaro, M.A., Castro, J.T.P., Martha, L.F. and Bittencourt, T.N. (2003), "Fatigue life and path predictions in generic 2D structural components", *Eng. Fract. Mech.*, **70**, 1259-1279.
- Newman, J.C. (1992), *FASTRAN II: A Fatigue Crack Growth Structural Analysis Program*, NASA TM-104159.
- Newman, J.C. (1981), "A crack closure model for predicting fatigue crack growth under aircraft spectrum loading", *Methods and Models for predicting Fatigue Crack Growth Under Random Loading* (Eds. Chang and Hudson), ASTM STP 748, American Society for Testing and Materials, 53-84.
- Paluszny, A. and Matthäi, K.S. (2009), "Numerical modeling of discrete multi-crack growth applied to pattern formation in geological brittle media", *Int. J. Solids Struct.*, **46**, 3383-3397.
- Paris, P.C. and Erdogan, F. (1960), "A critical analysis of crack propagation laws", *J. Basic Eng.*, **85**, 528-534.
- Phongthanapanich, S. and Dechaumphai, P. (2004), "Adaptive Delaunay triangulation with object-oriented programming for crack propagation analysis", *Finite Elem. Anal. Des.*, **40**, 1753-1771.
- Tanaka, K. (1974) "Fatigue crack propagation from a crack inclined to the cyclic tensile axis", *Eng. Fract. Mech.*, **6**, 493-507.

- Tilbrook, M.T., Reimanis, I.E., Rozenburg, K. and Hoffman, M. (2005), "Effects of plastic yielding on crack propagation near ductile/brittle interfaces", *Acta Mater.*, **53**, 3935-3949.
- Weertman, J. (1966), "Rate of growth of fatigue cracks calculated from the theory of indefinitesimal dislocations distributed on a plane", *Int. J. Fract. Mech.*, **2**, 460-467.
- Yan, X. (2007), "Automated simulation of fatigue crack propagation for two-dimensional linear elastic fracture mechanics problems by boundary element method", *Eng. Fract. Mech.*, **74**, 1727-1738.
- Zhao, T., Zhang, J. and Jiang, Y. (2008), "A study of fatigue crack growth of 7075-T651 aluminum alloy", *Int. J. Fatigue*, **30**, 1169-1180.
- Zienkiewicz, O.C., Taylor, R.L. and Zhu, J.Z. (2005), *The Finite Element Method: Its Basis and Fundamental*, Elsevier Butterworth-Heinemann, Burlington.